Bull Volcanol (2013) 75:681
DOI 10.1007/s00445-012-0681-2

RESEARCH ARTICLE

Evolution of crust- and core-dominated lava flows using scaling analysis

Angelo Castruccio · A. C. Rust · R. S. J. Sparks

Received: 23 August 2012 / Accepted: 18 December 2012 / Published online: 9 January 2013

Abstract We present a simple tool to evaluate the dominant dynamical regime of a lava flow and to estimate the order of magnitude of the main rheological parameter (viscosity or yield strength) controlling the length of the lava flow with time. We consider three dynamical regimes: a Newtonian viscous regime, a yield strength-dominated regime and a crust-dominated regime. For each of these regimes, we present a scaling analysis to derive relationships between front position and time, emitted volume, slope, width of the flow and rheological properties. We apply the resulting equations to published data from eruptions of 10 lava flows with a range of compositions and conditions. Comparisons of the fits of the models to the data reveal that short-lived, high effusion rate eruptions are dominated by the internal viscosity of the lava, whereas low effusion rate or long-lived eruptions are dominated by the yield strength in the growing crust. Finally, blocky lavas with very high initial crystal contents are dominated by the internal yield strength. The evolution of some flows can be approximated with only two viscosity values: an early low lava viscosity stage and a later higher viscosity stage. The increase in viscosity is attributed to the initial disequilibrium conditions of the magma at the vent with further degassing and cooling triggering crystallisation of the lava flow. For yield strength-dominated flows yield strength is always within an order of magnitude of 10^5 Pa. This study provides a practical framework for predicting the evolution of the length of lava flows from estimates of the crystal content of the erupting lava and its effusion rate.

Keywords Lava flows · Scaling analysis · Yield strength · Lava crust · Effusion rate

Editorial responsibility: A. Harris and S. Calvari

A. Castruccio · A. C. Rust · R. S. J. Sparks
Department of Earth Sciences, University of Bristol, Wills Memorial Building, Queen's Road,
Bristol BS8 1RJ, UK

A. Castruccio (✉)
Departamento de Geología, Universidad de Chile, Plaza Ercilla 803, Casilla 13518,
Santiago, Chile
e-mail: acastruc@ing.uchile.cl

Introduction

The evolution of a lava flow depends on many factors including the effusion rate, the underlying topography, and the rheology of the lava, which is modified by degassing and cooling. Further complexities arise from the formation of levées, evolution of a cooled crust, development of lava tubes and inflation processes. Despite these complexities, lava flow evolution can often be usefully approximated with simple models. The simplest way to treat lava flows is as Newtonian flows (e.g. Huppert et al. 1982; Tallarico and Dragoni 1999). More complex rheologies include the Bingham model (Hulme 1974; Dragoni et al. 1986) or the Herschel–Bulkley model (Balmforth and Craster 2000). Previous studies have focused mainly on the factors that control the final length of lava flows. Walker (1973) was the first to postulate that the final length is primarily controlled by effusion rate. Later, Pinkerton and Wilson (1994) refined this concept and evaluated other factors such as terrain slope, rheology and cooling. More recently, Harris and Rowland (2009) reviewed the role of heat loss and its relation with the effusion rate in the control of lava flow length. An effective and simple approach for the determination of the maximum flow length is the use of the Gratz number (Pinkerton and Sparks 1976; Guest et al. 1987; Pinkerton and Wilson 1994), which is a dimensionless parameter that quantifies the relative rates of advection and conductive cooling.

Numerical models are still unable to simulate all the complex phenomena of lava flows and some simplifications must be made, such as limiting to 1D or 2D, neglecting the influence of the crust on the dynamics and assuming idealised

rheologies. For example, computer simulations assuming a Bingham lava rheology are effective in characterising the evolution of lava flows in specific eruptions (Ishihara et al. 1992; Miyamoto and Sasaki 1997; Harris and Rowland 2001; Del Negro et al. 2008). However, rheological parameters (viscosity and yield strength) need to be calibrated, and it can be difficult to obtain a general relationship between such parameters and conditions like temperature and crystal content. Yield strength has proved to be especially difficult to parameterise and formulations between yield strength and crystal content (Gay et al. 1969; Ryerson et al. 1988; Dragoni and Tallarico 1994; Zhou et al. 1995) can vary by orders of magnitude for the same conditions. However, estimates of the yield strengths of lava domes and flows based on their morphologies and flow rates are relatively consistent. Blake (1992) proposed a model for lava domes controlled by the internal yield strength and found values of ~10^4–10^5 Pa for domes of andesite to rhyolite compositions. Fink and Griffiths (1998) inferred similar values for a set of 15 domes from dome morphology and flow rate data. Pinkerton and Wilson (1994) summarised the values of viscosity and yield strength for lava flows of basaltic to rhyolitic composition with a maximum yield strength of 10^5 Pa for all compositions, suggesting an upper bound for the maximum attainable yield strength for lavas.

In this work, we investigated, through a scaling analysis, three different regimes that can control the dynamics of a lava flow, namely a Newtonian viscosity, a yield strength in the whole flow (YS model) and a yield strength in a diffusively growing external crust (YSC model). Our motivation comes from observations that suggest that sometimes lava flow advance is mainly controlled by factors other than the internal viscosity. For example, a common occurrence in Etna lava flows is the stopping of the front flow, followed by inflation, and finally by a breakage in the crust with the formation of a secondary flow, composed of hot and fluid internal lava (Pinkerton and Sparks 1976; Dragoni and Tallarico 1996; Favalli et al. 2009). Another example is the 1988–1989 Lonquimay eruption, Chile, where temperatures of ~1,040 °C were measured in the interior of the flow front, more than 9 km from the vent and after more than 100 days of eruption (Moreno and Gardeweg 1989). Despite this high internal temperature, close to the eruption temperature, the apparent viscosity, determined from the advance of the lava, was calculated to be as high as ~10^9 Pas (Naranjo et al. 1992), suggesting a control other than the core viscosity.

Our analysis presented here follows the previous works on Bingham fluids of Hulme (1974) and Dragoni et al. (1986) and the ideas about scaling of Huppert (1982), Griffiths and Fink (1993), Kerr and Lyman (2007) and Takagi and Huppert (2010). From this analysis, we present relationships between flow front position and rheology and test them on published data from 10 lava flows with a range of compositions and initial conditions. All the eruptions considered generated simple lava flows according to the definition of Walker (1973). We use the evolution of the flow front position, emitted volume, terrain slope and flow width data to determine the flow regime and estimate the lava rheology (viscosity and yield strength), which we compare to rheology determined by other methods. The study focuses on inverting field data for flow regime and rheology, but it also provides a method for predicting flow evolution if the effusion rate is known.

Theory of lava flows on a slope

We consider a free surface two-dimensional laminar flow down a slope of lava with a Bingham rheology:

$$\tau = \sigma_y + \mu\dot{\gamma} \tag{1}$$

where τ is the applied shear stress, $\dot{\gamma}$ is the strain rate, μ is the plastic viscosity and σ_y is the yield strength. The flow is driven by gravity and the shear stress in the lava flow is:

$$\tau = z\rho g \sin\beta \tag{2}$$

where z is the coordinate perpendicular to the surface with the origin at the top of the flow, ρ is the lava density, g is gravity and β is the terrain slope. Considering that the shear rate inside the flow is:

$$\dot{\gamma} = -\frac{\mathrm{du}}{\mathrm{dz}} \tag{3}$$

where u is the flow velocity, the average velocity, $\overline{u}$, is:

$$\overline{u} = \frac{H^2\rho g \sin\beta}{3\mu}\left(1 - \frac{3h_c}{2H} + \frac{h_c^3}{2H^3}\right) \tag{4}$$

where $h_c = \frac{\sigma_y}{\rho g \sin\beta}$ is the thickness of the plug region (Hulme 1974; Dragoni et al. 1986), and H is the height of the flow. For the velocity of a flow with a more complex Herschel–Bulkley rheology, see Castruccio et al. (2010).

Assuming a rectangular channel, the effusion rate is

$$\frac{\mathrm{dV}}{\mathrm{dt}} = \overline{u}\, WH \tag{5}$$

where V is the volume and $\mathrm{d}V/\mathrm{d}t$ is the instantaneous variation of volume or effusion rate. W is the width of the flow. Combining Eqs. (4) and (5) gives:

$$\frac{\mathrm{dV}}{\mathrm{dt}} = \frac{H^3 W\rho g \sin\beta}{3\mu}\left(1 - \frac{3h_c}{2H} + \frac{h_c^3}{2H^3}\right) \tag{6}$$

Thus, if we know the effusion rate, the width of the flow and its rheology, we can solve Eq. (6) to obtain the height and, consequently, the velocity of the flow (Dragoni et al. 1986).

Scaling analysis

In the following analysis, we assume that the driving force of the flow is due to gravity acceleration, but we do not consider the pressure gradient due to differences in height through the flow. By setting the mass of the flow equal to $V\rho$ and the acceleration equal to $g\sin\beta$, the driving force F_D is proportional to:

$$F_D \sim V\rho g \sin\beta \tag{7}$$

For the stopping force, we considered three cases. First, we assume a Newtonian viscosity in the flow. Second, we consider the case when the flow is controlled by a yield strength in the whole flow, and finally, we consider a yield strength in a diffusively growing crust (Fig. 1).

Newtonian case (N)

For a Newtonian lava, the retarding force will be proportional to $\mu\dot{\gamma}$, where μ is the viscosity and $\dot{\gamma}$ is the strain rate and is proportional to U/H, where U is the characteristic velocity of the flow and H is the thickness. As the viscous forces act over an area equal to the base of the flow, which is proportional to LW, where L is the length of the flow, we can write the retarding force as:

$$F_R \sim \mu \frac{U}{H} LW \tag{8}$$

Combining Eqs. (7) and (8) and scaling U as $\sim L/t$ and $V \sim LHW$ we arrive to:

$$L = C_1 \left(\frac{V^2 \rho g \sin\beta t}{\mu W^2} \right)^{1/3} \tag{9}$$

where C_1 is a constant. Note that we can arrive to the same result from Eq. (6) if we integrate over t, set $\sigma_y = 0$ and assume $V \sim LHW$.

The evolution with time of the volume V can be modelled in different forms. For example Huppert et al. (1982) and Takagi and Huppert (2010) used a power-law relationship in the form of:

$$V = Qt^{\alpha} \tag{10}$$

where Q and α are constants. If $\alpha=1$, the effusion rate is constant; if $0<\alpha<1$, the effusion rate decreases with time; and if $\alpha>1$, the effusion rate increases with time. For instance, replacing Eq. (10) in Eq. (9) gives:

$$L \sim \left(\frac{Q^2 \rho g \sin\beta}{\mu W^2} \right)^{1/3} t^{\frac{2\alpha+1}{3}} \tag{11}$$

This result was obtained by Lister (1992) and was tested by Takagi and Huppert (2010) for the evolution of lava flows at three volcanoes.

The direct application of Eq. 9 may not be appropriate due to changes in the terrain slope, width of the flow and lava viscosity during an effusive eruption; furthermore, the

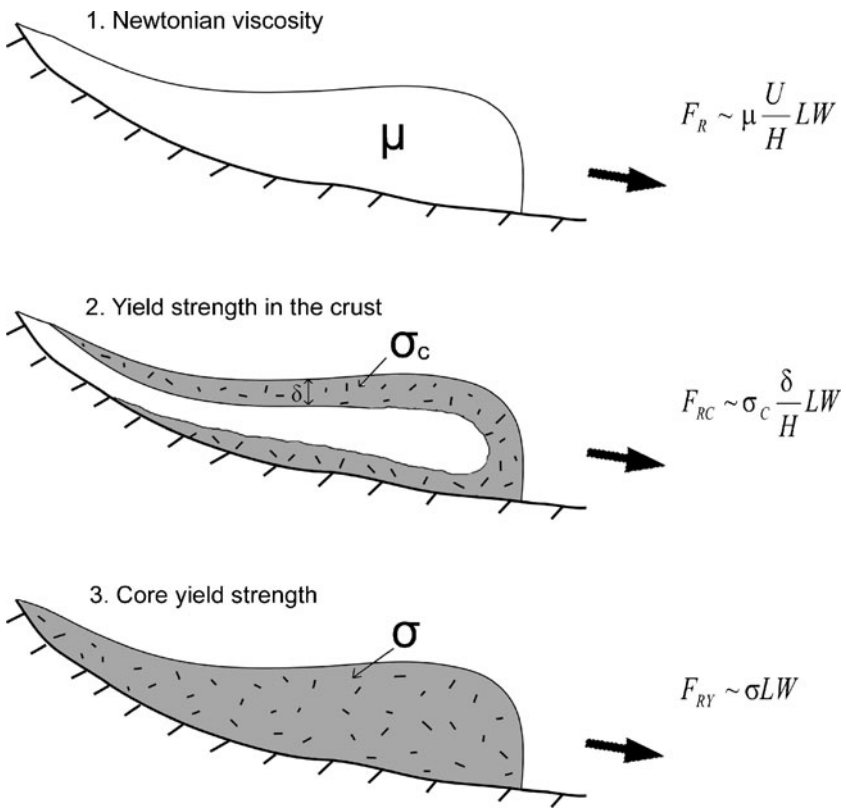

Fig. 1 Cartoon showing the three regimes analysed in this work. Also shown are the retarding forces (F_R) for each case. The yield strength in the crust cartoon shows crusts at the top and base of the flow; the scaling analysis approach would be the same if only considered a single crust on the top of the flow

change in volume with time might not be well approximated by a simple equation such as Eq. 10. Additionally, Lipman and Banks (1987) described three parts for the lava flows of the 1984 Mauna Loa eruption: (a) a channelised section with stationary levees, where the lava is transported efficiently to the front; (b) a transition zone; and (c) a dispersed flow section at the front without channel or levees and where the lengthening of the flow takes place. These divisions have been recognised in many others flows (Lonquimay, 1988–1990, Naranjo et al. 1992; Puu Oo, 1983, Wolfe et al. 1988; Etna, 2001, Favalli et al. 2009). In addition, Borgia et al. (1983) observed that the dynamics of lava flows at Arenal volcano were controlled by frontal processes and the flow stopped when the lava supply from the channel to the front ceased. According to this evidence, the advance of a lava flow can be modelled as the advance of the flow front fed by lava from the channelised section and we propose the following formulation for its advance:

$$L = C_1 \sum_{i=1}^{n} \left(\frac{V_i^2 \rho g \sin \beta_i t_i}{\mu_i W_i^2} \right)^{1/3} \tag{12}$$

where V_i is the volume added in each step from the channel zone to the front (that can be equal to the erupted volume at the vent, but not necessarily), β_i is the terrain slope at the front, t_i is the time interval between each step, and μ_i and W_i are the viscosity and width of the front zone. Equation (12) will be equal to Eq. (9) when dV/dt is constant and the width, viscosity and slope do not change.

Yield strength in the core (YS)

Next, we consider the case where the stresses driving flow just exceed the yield strength. A force is evaluated for the bulk flow and converted to a stress by dividing by the cross-section. This case is analysed by equating the yield stress and driving stress. The resistive force acting on the whole flow is :

$$F_{RY} \sim \sigma_y LW \tag{13}$$

Combining Eqs. (7) and (13) and using $V \sim LHW$ we get:

$$L = C_2 \frac{V \rho g \sin \beta}{\sigma_y W} \tag{14}$$

Writing this equation in a summation form, adding material to the flow front at each step, we get:

$$L = C_2 \sum_{i=1}^{n} \left(\frac{V_i \rho g \sin \beta_i}{\sigma_{yi} W_i} \right) \tag{15}$$

comparable to Eq. (12) for the Newtonian case.

Yield strength in a growing crust (YSC)

In the third case, we assume that the flow is slowing down due to the yield strength of a crust growing by conductive cooling, with a thickness δ:

$$\delta \sim \sqrt{\kappa t} \tag{16}$$

where κ is the thermal diffusivity of the lava, with a value of $\sim 10^{-6}$ m^2/s (Pinkerton and Sparks 1976; Kerr and Lyman 2007). The retarding force can be written as:

$$F_{RC} \sim \sigma_C \frac{\delta}{H} LW \tag{17}$$

where σ_C is the yield strength of the crust. Equating Eqs. (7) and (17), we get:

$$L = C_3 \left(\frac{V^2 \rho g \sin \beta}{W^2 \sigma_c \sqrt{\kappa t}} \right)^{1/2} \tag{18}$$

The cumulative version of Eq. (18) is:

$$L = C_3 \sum_{i=1}^{n} \left(\frac{V_i^2 \rho g \sin \beta_i}{W_i^2 \sigma_{ci} \sqrt{\kappa t}} \right)^{1/2} \tag{19}$$

Lava flow eruptions dataset

We selected 10 lava flows from six volcanoes: Pu´u ´O´o, 1983–1984 (four selected events, Wolfe et al. 1988); Mauna Loa 1984 (Lipman and Banks 1987); Lonquimay, 1988–1989 (Naranjo et al. 1992); Etna 2001 (Behncke and Neri 2003; Coltelli et al. 2007); Etna 2006 (Vicari et al. 2009); Colima 1998–1999 (Navarro-Ochoa et al. 2002) and Santiaguito 1999–2002 (Harris et al. 2004). We chose these eruptions because they were composed of a simple flow (at least at the beginning stages), and the evolution of the flow front and volume erupted are well documented. The duration of the lava flow emplacement ranges from 1 day to 2 years, the final length from 3 to 26 km, and the erupted volume from 3.7 to 212× 10^6 m^3 (Table 1). The composition of the erupted products ranges from basaltic to dacitic and the terrain slopes vary between 1 and 35° (Fig. 2).

The erupted volume as a function of time (effusion rate) is the most difficult parameter to evaluate due to the diversity of methods employed, their typical poor precision and the uncertainty of how much of the calculated flow rate effectively contributes to the flow advance due to mass losses derived from solidification or branching of the main flow. According to Harris et al. (2007), errors can be as high as 50 %. Consequently, for every eruption, we checked that the flow thicknesses calculated from length, width and volume erupted are in the range of the actual values, and we

Table 1 Eruptions and flow parameters used in the analysis

Volcano	Year	Duration (days)	Final length (km)	Final volume ($\times 10^6$ m^3)	Method to obtain volume	Thickness data	Chemical composition	Morphology	Source
Mauna Loa (flow 1)	1984	7.5	25	54	Integration of flow rate calculated using velocity and cross section of the flow	Some points	Basaltic	Aa—Pahoehoe	Lipman and Banks (1987)
Puu-Oo (episodes 4, 5, 11, 17)	1983–1984	1.1–4.2	7.6–10.7	8.3–11.6	Area of the flow by mean thickness	Yes	Basaltic	Aa—Pahoehoe	Wolfe et al. (1988)
Etna	2001	8	6.9	15	DEM substraction	Some points	Trachybasaltic	Aa	Coltelli et al. (2007)
Etna	2006	10	4.2	3.8	Integration of flow rate calculated using heat measurements by satellite	No	Trachybasaltic	Aa	Vicari et al. (2009)
Lonquimay	1988–1989	330	10.2	212	Area of the flow by mean thickness	Yes	Andesitic	Aa—Blocky	Naranjo et al. (1992)
Colima	1998–1999	79	3.8	40	Not stated	Proximal and distal ends	Andesitic	Blocky	Navarro-Ochoa et al. (2002)
Santiaguito	1999–2001	561	4.1	27.7	Integration of flow rate calculated using heat measurements by satellite	Some points	Andesitic	Blocky	Harris et al. (2004)

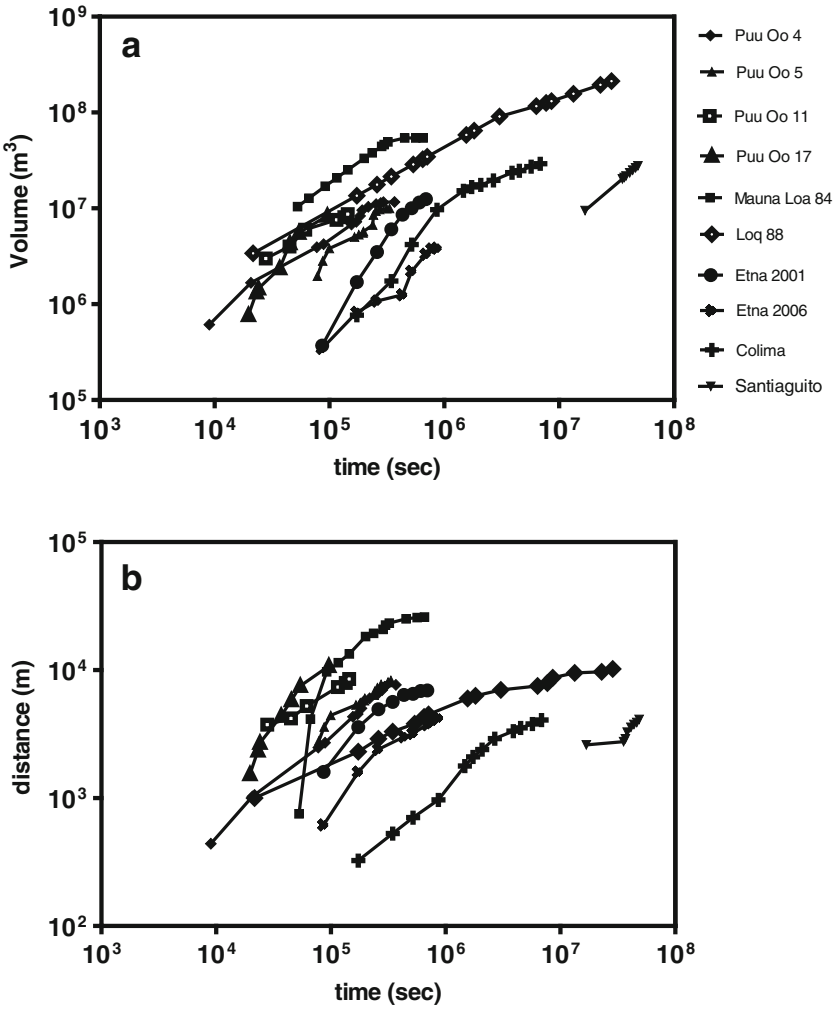

Fig. 2 Erupted volume (**a**) and front position (**b**) as a function of time for the eruptions analysed in this work. See Table 1 for data sources and details

discarded flows where branching was complex. Common methods for estimating rate of volume added to a lava flow include periodic measurements of the dimensions of the lava body, measurements of mean velocity of the flow in an open channel and the cross-section in order to obtain the effusion rate, and remote sensing techniques such as thermal data from satellites (Harris et al. 2007). Table 1 indicates the method and data source for each lava flow studied here. We used a mean density of 2,500 kg/m^3 for all lava flows. The widths of the flows were taken from published maps of the lava flows at many positions. These values may overestimate the actual value of the width due to subsequent overflows or levee formation.

Application of models to lava flow emplacement

In this section, we will analyse the data from these eruptions using the equations developed in "Theory of lava flows on a slope." For each eruption, we fitted the front position versus time data with the three models by minimizing the squared residuals in flow front position. Our goal is to determine which model best represents the available data and to estimate the order of magnitude of the viscosity or yield strength of the lava accordingly. The models of all three dynamical regimes (Newtonian, YSC and YS) can be perfectly fit to the data if the rheology is permitted to change at every data point (although the result may imply unrealistic flow thicknesses). However, for the models to be of practical use, we apply the principle of parsimony and so we seek models that fit the data with the fewest changes in rheology and dynamical regimes during an eruption. We began by determining the best fit where the rheology of the lava is constant and the flow regime is the same for the whole eruption. If none of these provided an adequate fit then either the rheology or the dynamical regime or both were allowed to change only once during an eruption, thus dividing it into two stages.

We modelled the evolution of the lava flows with the following approach: for every eruption, we applied each of the three models (Newtonian, YSC and YC), using the cumulative Eqs. (12), (15) and (19), trying to use as few rheological parameters as possible. The use of a single rheology for the entire duration of the flow is not adequate for most flows, with errors as high as 30 % in the predicted length. However, using two rheologies, namely an initial viscosity or yield strength for the first portion of the flow and then a higher one for the remainder of the eruption, the modelling is much better, with errors <3–5 % in the predicted final length. For some eruptions, the best fit is achieved using an initial Newtonian regime and then a YSC regime.

In the Lonquimay eruption case, the terrain slope and the flow width were approximately constant, and the discharge rate is well described by power-law relationships with time (Fig. 5a). This makes it feasible to fit the flow advance data with noncumulative Eqs. (11), (14), and (18) replacing V with Eq. (10), similar to Kerr and Lyman (2007), and we compare the results (dynamical model and rheology) with those determined from fits with the cumulative versions of these equations.

Pu´u ´O´o, 1983–1984

Pu´u ´O´o is an eruptive vent forming part of the Kilauea's east rift zone in Hawaii. At the beginning of 1983, it started an eruptive cycle that during the first 17 months produced 19 episodes of vigorous activity alternated with longer repose episodes (Wolfe et al. 1988). The eruptive episodes generated lava flows of basaltic composition with both pahoehoe and 'a'a morphologies. The erupted lavas had an initial temperature of 1,098–1,147 °C. For this study, we selected episodes 4, 5, 11, and 17 for our analysis because these episodes represent well the initial stages (episodes 4 and 5), where the crystal content was high and the effusion rate low compared with the latter stages (episodes 11 and 17) where the effusion rate was higher and the crystal content lower (Wolfe et al. 1988). There was branching of all of the flows, especially near the vent and only the volume in the main channel was included in this study. Figure 3 shows the evolution of the flow front for the four episodes and the fits using Eqs. (12), (15) and (19) with two rheological parameters in each case. The best fit for the initial stages is the Newtonian model. For latter stages (the second portion for each flow), the Newtonian model is marginally the best fit but this is not significant given the uncertainties in the input parameters. The calculated viscosities for the initial stages are $1.0–2.0\times10^5$ Pas (first day) for episodes 4 and 5, and $1.8–2.5\times10^4$ Pas (first half day) for episodes 11 and 17. For latter stages, the viscosities are $\sim4.5\times10^6$ Pas for flows 4 and 5 and $1.9–2.5\times10^5$ Pas for flows 11 and 17. These results indicate that viscosities of episode 4 and 5 are one order of magnitude higher than episodes 11 and 17. This is consistent with the observations made by Wolfe et al. (1988) of lower phenocryst contents and higher temperatures in the latter episodes. The best-fit two-stage YSC models (using the same division of stages as for the Newtonian model fitting) give a crust yield strength of $2.4–3.5\times10^4$ Pa in the initial stage and $2.2–2.7\times10^5$ Pa for the later stage for episodes 4 and 5, and $1.1–2.4\times10^4$ Pa in the initial stage and $0.2–1.1\times10^5$ Pa for the later stages of episodes 11 and 17. Values for the yield strength for the best-fit two-stage YS model are $1.5–2.7\times10^3$ Pa in the initial stage and $1.8–1.9\times10^4$ Pa in the later stage for episodes 4 and 5; for episodes 11 and 17, the values are $0.9–1.6\times10^3$ Pa in the initial stage and $2.3–7.5\times10^3$ Pa in the later stage (Table 2). Episodes 5, 11, and 17 data are well described by these

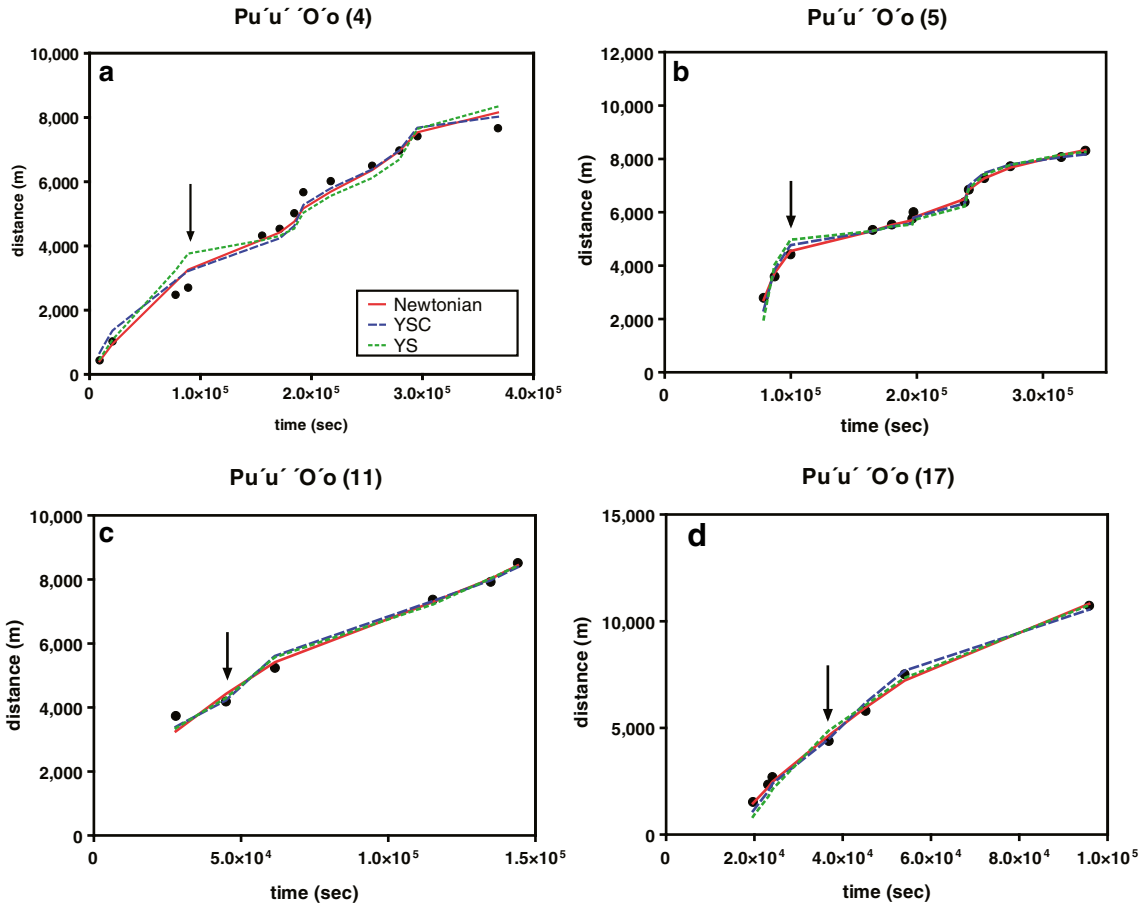

Fig. 3 Flow length (L) as a function of time (*circles*) for four episodes of the 1983 Pu´u´ ´O´o eruption. The *lines* are the best fits using Eqs. (12), (15) and (19). *Arrows* indicate the point delimiting the two stages in the flow and thus indicates where the rheology changes in the fits of the models to the data

models, whereas some points from episode 4 do not fit well to any of the simple models applied here. We attribute this to sudden changes in the discharge rate and slope: the complexities of these transient effects are not captured by the models.

Mauna Loa, 1984

The 1984 eruption started on 25 March at the summit caldera and the northeast rift zone (Lipman and Banks 1987). By 29 March, flow 1 reached 25 km from its source vent. Lava flows were mainly ‘a’a type, with pahoehoe morphology only in the first 2 km. After 4 days, a major branching occurred 13 km from the vent forming the flow 1A (extensively studied by Pinkerton and Wilson 1994). We focus on the evolution of flow 1 up to the initiation of flow 1A. Our analysis shows that initially all three models adequately describe the front evolution (Fig. 4). For later stages, the YSC and YS fit the data slightly better. The viscosities for the best fit of the Newtonian model are 6.0×10^4 Pas for the first 2 days and then a viscosity of 2.3×10^6 Pas for the rest of the flow, which are in the range of viscosities we inferred for the Pu´u ´O´o episodes. The yield strength in the crust model can describe the evolution of the front with an initial strength of 4.4×10^4 Pa and a subsequent strength of 2.3×10^5 Pa. The YS model fits the data with an initial yield strength of 5×10^3 Pa and a yield strength of 1.2×10^4 Pa for later stages (Table 2).

Lonquimay, 1988–1989

The 1988–1989 Lonquimay eruption began on 25 December 1988 on the NE flank of the volcano, forming a cinder cone almost 200 m high. The morphology of the andesite flow has a transitional character between ‘a’a and blocky (Moreno and Gardeweg 1989). Near the beginning of the eruption, there was a small branch directed to the north, which was not included in our analysis. The simplest model that adequately describes the evolution of the flow is the YSC with a constant crust yield strength of 4.7×10^5 Pa (Fig. 5a). Both Newtonian and YS models need two rheological parameters to fit the data adequately; even with two fit parameters (i.e. separate viscosities for early and late stages of the flow), the Newtonian model gives a poorer fit

Table 2 Calculated values for viscosities and yield strength to fit the data of the eruptions using the three models described in the text

	Newtonian		Newtonian-YSC		Newtonian-YS		YSC		YS	
	Viscosity 1 (Pas)	Viscosity 2 (Pas)	Viscosity 1 (Pas)	Yield strength 1 (Pas)	Viscosity 1 (Pas)	Yield strength (Pa)	YS 1 (Pa)	YS 2 (Pa)	YS 1 (Pa)	YS 2 (Pa)
Mauna Loa, Episode 1A	6.13E+04	2.37E+06					4.40E+04	2.28E+05	5.06E+03	1.28E+04
Puu Oo										
Episode 4	1.32E+05	4.85E+06					2.48E+04	2.22E+05	1.55E+03	1.82E+04
Episode 5	2.10E+05	4.64E+06					3.54E+04	2.70E+05	2.76E+03	1.92E+04
Episode 11	1.81E+04	1.97E+05					1.16E+04	2.44E+04	8.91E+02	2.31E+03
Episode 17	2.55E+04	2.60E+05					2.41E+04	1.14E+05	1.61E+03	7.58E+03
Etna 2001	3.89E+06	2.36E+08	4.49E+06	1.09E+06	4.56E+06	4.57E+04				
Etna 2006	1.31E+07	4.16E+08	2.14E+07	1.35E+06	2.10E+07	5.82E+04				
Lonquimay 1988–90	1.96E+07	1.50E+10					4.71E+05		1.65E+04	9.05E+04
Colima 1999–2000	6.00E+09						4.23E+06		1.61E+05	
Santiaguito	3.75E+10	5.51E+11					6.70E+05		1.29E+05	

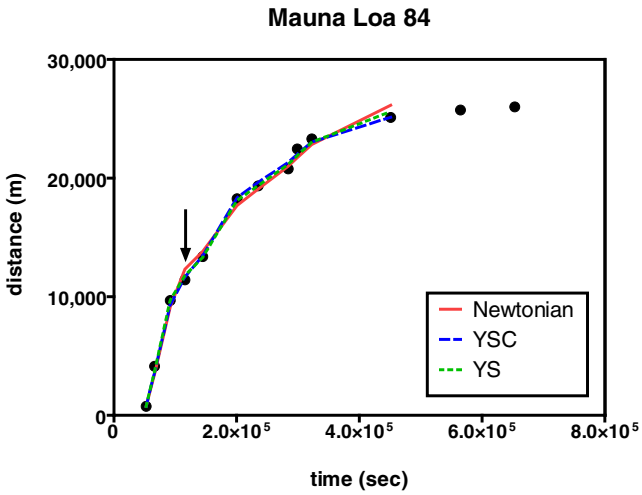

Fig. 4 Flow length (L) as a function of time (*circles*) for the flow 1 of the 1984 eruption of Mauna Loa. *Arrow* indicates the point where the rheology changes. The last two points are not analysed due to uncertainties in flow rate (breakage and generation of flow 1A).

than the YSC with a single yield strength. For this particular eruption, the erupted volume as a function of time can be described by two power law relationships, one for the first 21 days (time exponent, α=0.66) and a second (α=0.39) for the rest of the eruption (Fig. 5b). The terrain slope and flow width are approximately constant and can be set to β=3.5° (Naranjo et al. 1992) and W=600 m respectively. Consequently, the evolution of the flow front can also be modelled using continuous Eqs. 11, 14 or 18. Using the α, β and W values listed above, these equations predict power-law relationships between front position (L) and time (t): the Newtonian model predicts time exponents for the front evolution of 0.77 (first 21 days) and 0.59 (after 21 days), the yield strength in the core model predicts 0.66 and 0.39 and the yield strength in the crust model predicts 0.41 and 0.14. The power-law fit to the field $L(t)$ data has time exponents of 0.42 and 0.17 for the first 21 days and subsequent days, respectively (Fig. 5c); thus, the yield strength in the crust model is clearly the best match to the actual flow front evolution. The calculated yield strength [a fitting parameter of the YSC model; Eq. (18) with prescribed V–t power-law relationship] is 2.8×10^5 Pa and the modelled advance is shown in Fig. 5c. This value is lower than the estimate using the accumulative equation (Eq. 19) but is the same order of magnitude. The discrepancy is related to the different assumptions implied by Eqs. (18) and (19). Equation (18) assumes that the whole flow is moving and adjusting (e.g., H changes) to changes in Q, and the crustal strength is acting over the entire flow, while Eq. (19) assumes that once established, the lava flow geometry does not change, and all the action is at the flow front. Reports of the eruption (Moreno and Gardeweg 1989) suggest that the flow motion is

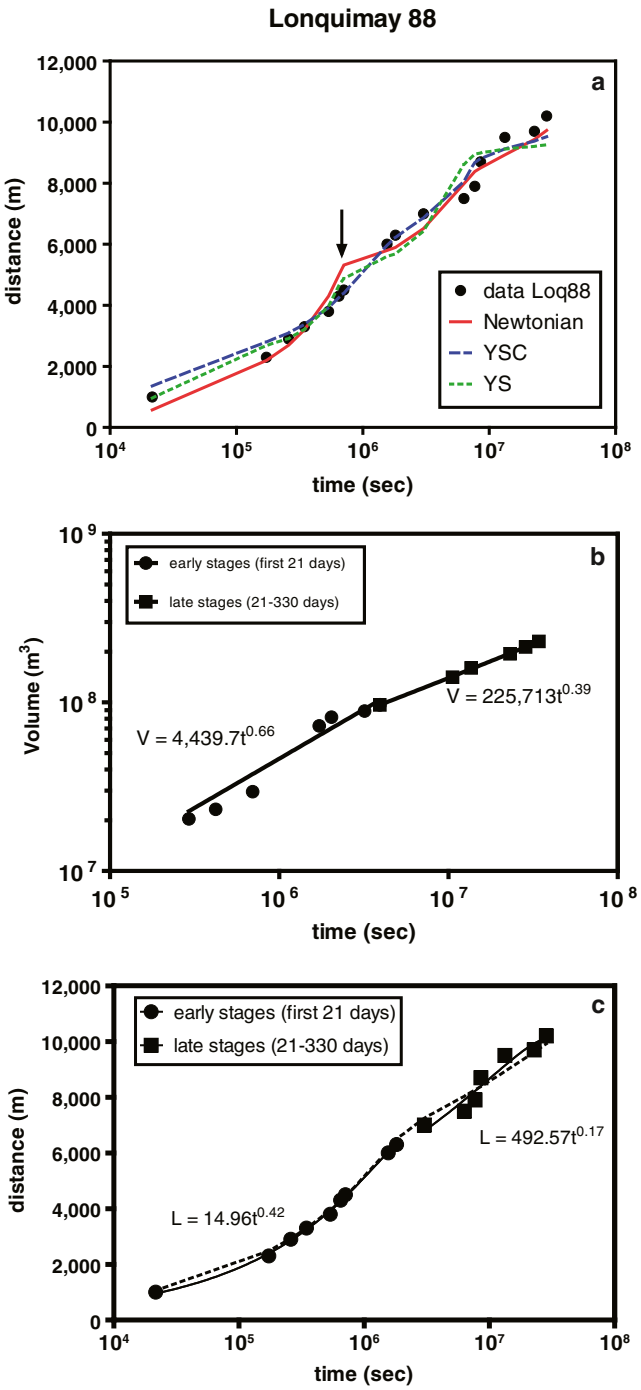

Fig. 5 **a** Flow length (L) as a function of time (*circles*) for the 1988–1990 Lonquimay eruption and the best fit with the three models. The *arrow* indicates the point where the rheology changes for Newtonian and YSC models; the YS model is for a constant rheology (i.e., constant yield strength). **b** Erupted volume as a function of time for the 1988–1989 Lonquimay eruption. The *lines* are the fit to data for the early (*circles*) and late (*squares*) stages of the eruption. **c** Best fit (*dashed line*) for the flow advance using Eq. 18 with W=600 m and β=3°. The best fit is for a growing crust with a yield strength of 2.8×10^5 Pa

concentrated at the front, with a central channel feeding the front with new lava. Kerr and Lyman (2007) estimated a higher yield strength with a value of 2 MPa for the same flow with a similar model involving a yield strength in a thickening crust. However, they did not include the effect of slope and assumed that volume discharge rate decreased exponentially with time.

Etna, 2001

The 2001 eruption lasted from 17 July until 9 August. It generated seven main flows on the S and E flanks of the volcano (Behncke and Neri 2003). In our analysis, we focused on the flow F4 according to the nomenclature of Behncke and Neri (2003) (LFS1 according to Coltelli et al. 2007). The flow has an 'a'a morphology and a trachybasalt composition, with a maximum length of 6.4 km. We only use data up to 25 July because after this date the flow was complicated by both the formation of major branches and the flow of lava on top of lava from earlier in the eruption. Our analysis reveals that the best fit using two rheological parameters is the Newtonian model (Fig. 6a). However, the calculated thicknesses in the latter stage of the flow are much greater than the field measurements (Fig. 6b). The best solution to fit both the front evolution and flow thickness is an initial Newtonian viscosity for the first 3 days and then the YSC model for the rest of the flow. If we use the Newtonian model with a change in viscosity after 3 days, then the initial viscosity is 3.8×10^6 Pas and the second viscosity is 2.4×10^8 Pas. The two stage model with Newtonian behaviour followed by the crustal yield strength model gives an initial viscosity of 4.5×10^6 Pas and a crustal strength of 1.0×10^6 Pa. (Note that the initial viscosity is slightly higher than in the first stage of the best fit for the two Newtonian viscosities case. This is due to the fitting procedure, which requires that the position at the end of the Newtonian stage matches the position at the start of the YSC stage.) A fit with a Newtonian-then-Yield strength in the core is also shown in Fig. 6a, but the calculated value of the strength (4.5×10^4 Pa) is too low to dominate over the initial viscosity of 4.6×10^6 Pas (Table 2), as discussed in "Discussion."

Etna, 2006

The lava flow analysed here started on 14 July and stopped on 24 July, reaching more than 3 km from the vent through the Valle del Bove on the east flank of the volcano (Vicari et al. 2009). We did not include the small branch of the flow mapped by Vicari et al. (2009) on 21 July. The best fit to the $L(t)$ data using two rheological parameters is the model with two Newtonian viscosities with an initial viscosity of 1.3×10^7 Pas for the first 3 days and a second viscosity of 4.2×10^8 Pas for the rest of the flow (Fig. 6c). However, as for the Etna 2001 case, the calculated flow thicknesses associated with this model (up to 70 m) are much thicker than typical Etnean flows (although no thickness data were found for this particular eruption). Again, the best fit to the flow front

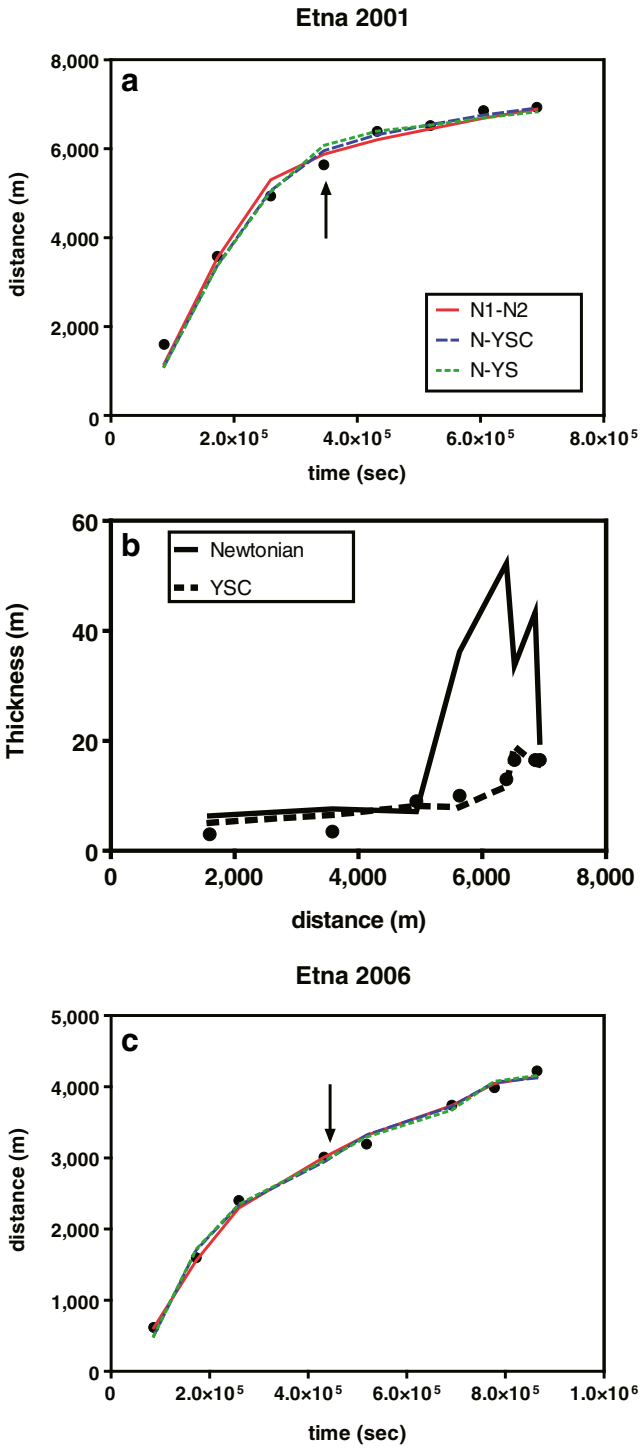

Fig. 6 **a** Flow length (L) as a function of time (*circles*) for the 2001 eruption of Etna. The two Newtonian (N1–N2) and Newtonian-then yield strength in the crust (N-YSC) models fit the data, but the calculated thicknesses are too high in the Newtonian case (**b**). The yield strength in the core model also fits the data with a calculated yield strength of 10^4 Pa. **c** Flow length data for the 2006 Etna eruption (legend is same as in **a**)

evolution data with feasible flow thicknesses is an initial Newtonian phase with viscosity of 4.5×10^6 Pas and a subsequent YSC phase with crustal strength of 1.1×10^6 Pa (Table 2).

Colima, 1998–1999

The eruption began in November with the emission of a dome at the summit. After the partial collapse of the dome and the generation of pyroclastic flows, a blocky, andesitic and crystal-rich lava flowed down the south flank of the volcano, reaching a maximum distance of 3.8 km (Navarro-Ochoa et al. 2002). There were two branches of the flow; we modelled the east branch that had a simpler geometry than the west branch. In this case, the best fit for the flow evolution and thickness is given by the core yield strength model with a single strength of 1.6×10^5 Pa (Fig. 7).

Santiaguito, 1999–2002

A blocky dacitic lava flow started to advance in July 1999, reaching a length of 3.7 km by January 2001 (Harris et al. 2004). During this period, the flow rate was ~0.5 m^3/s with heights up to 88 m. Here, we only modelled the advance between January 2000 and January 2001 because before these dates, the available data have large uncertainties. Figure 8 shows the best fits with the three models. The Newtonian model gives a viscosity of 3.8×10^{10} Pas, in agreement with the values given by Harris et al. (2004), based on the Jeffrey's equation. The YSC model gives a crust yield strength of 6.7×10^5 Pa and the YS model a core yield strength of 1.3×10^5 Pa (Table 2). Of the three models, the YS model fits slightly better, but this is not significant given parameter uncertainties and the poor fit of all three models around 3.8×10^7 s.

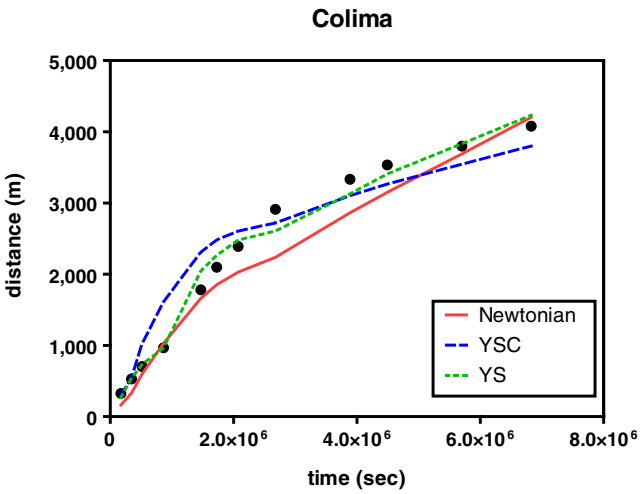

Fig. 7 Flow length (L) as a function of time (*circles*) for the East flow of the 1998–1999 eruption of Colima volcano. The best fit is the yield strength in the core model (YS) with a yield strength of 1.6×10^5 Pa

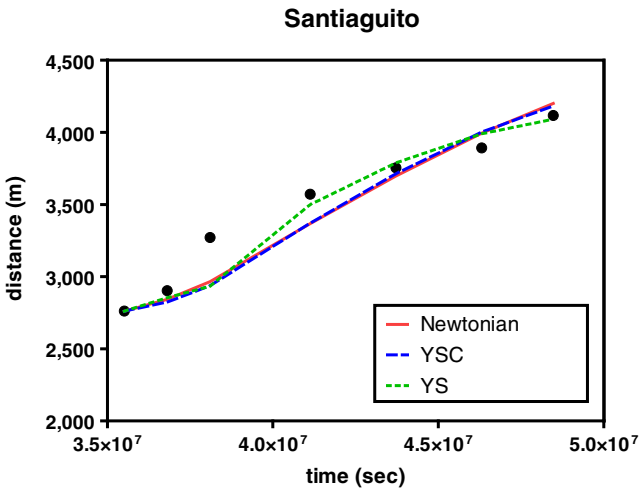

Fig. 8 Flow length (L) as a function of time (*circles*) for the lava flow of the 1999–2001 eruption of Santiaguito volcano. The best fit is with the yield strength in the core model (YS), using a yield strength of 1.3×10^5 Pa. The calculated viscosity for the Newtonian model is 3.8×10^{10} Pas, and the crustal yield strength is 6.7×10^5 Pa

Discussion

Dynamical regimes of lava flows

Our modelled flows suggest that for eruptions where the effusion rate is high (50–100 m^3/s), the duration is short (0.5–5 days) and the initial crystal content is relatively low (~1–10 % phenocrysts), such as the Hawaiian eruptions analysed in this study (Pu´u ´O´o, 1983–1984; stages 4, 5, 11 and 17), the dynamical regime is best described by the Newtonian model. In the initial stage (first day or half-day) of each of these flows, the Newtonian model clearly fits the data better than the two models that include a yield strength. In the later stage of each flow, however, the goodness of fit of the three models is similar and within the uncertainties of the input parameters. Thus, a "best" model cannot be discriminated on goodness-of-fit alone. Some features of these flows distinguish them from the other analysed flows where we found that yield strength is important, such as low thicknesses (typically <5 m) and exposed incandescent interiors (see photographs of the flows in Wolfe et al. 1988 and Lipman and Banks 1987) with a discontinuous or almost absent covering crust, even at distal parts. In addition, the calculated viscosity values are in excellent agreement with previous studies (see next subsection). On the other hand, calculated core yield strengths for the YS model are too low to dominate over the viscosity of the flow or are in disagreement with previous works, supporting a preference for the Newtonian regime for the Pu´u ´O´o flows studied here. However, the possibility of a yield strength in the crust control (YSC model) in the later stage of these flow, as fits the 1984 Mauna Loa eruption, cannot be discarded. In contrast to our results, Takagi and Huppert (2010) suggested that for some episodes of the Pu´u O´o eruption, a single (unspecified) viscosity can explain the advance of the flow, and thus heat loss does not have a significant effect on the front advance rate. However, they did not consider the total length of some flows (episode 4) as we did, or their linear fit of $L(t)$ data is not good in the initial stages of the flow (episode 17). Furthermore, they did not consider in detail variations in slope, width and flow rate of the flows, which we found account well for the nonlinearity of the L(t) data.

Lava flows at Etna and Lonquimay had lower (<20 m^3/s) effusion rates or longer durations (1 week–1 year) and usually greater degrees of crystallisation (phenocrysts plus microlites, Naranjo et al. 1992; Pinkerton and Norton 1995) than the Hawaiian lava flows analysed. Other differences include larger thicknesses (10–40 m, Naranjo et al. 1992; Favalli et al. 2009), less exposed interiors, with a more continuous external covering crust. Both two-stage Newtonian and Newtonian followed by YSC models fit the data for Etna well, but the calculated thicknesses are too high in the two-stage Newtonian case, suggesting a crustal control. Our calculated rheologies for the two stages of both the Etna 2001 and Lonquimay 1988 eruptions are consistent with the conclusion of Takagi and Huppert (2010) that the advance rates of these flows were affected by significant cooling and corresponding rheological change.

The Colima and Santiaguito lava flows are better modelled with the YS model using a single value for the yield strength. Both of these lava flows have a blocky flow morphology and are more silicic (andesitic to dacitic) and more crystalline than the other lava flows analysed, which are dominantly 'a'a in morphology. This suggests that cooling effects are less important to the advance rate of silicic blocky flows compared with basaltic 'a'a flows.

Viscosity magnitudes and crystallisation

The viscosity values we calculated for the Hawaiian lava flows are in excellent agreement with published values determined by others methods. Fink and Zimbelman (1986) calculated values of $0.2–8.6\times10^6$ Pas for the viscosity of the distal part of the episode 5 Pu´u ´O´o lava flow, using topography profiles of the final flow morphology and velocity and effusion rate data, bracketing the value of 4.6×10^6 Pas estimated in this study. Moore (1987) calculated values between $\sim1\times10^4$ Pas (proximal to the vent, flow 1) and $0.6–1\times10^7$ Pas (flow 1A) for the Mauna Loa eruption, using velocity profiles at the surface and flow dimensions, again in close agreement with our values of 6.1×10^4 Pas for early stages and 2.4×10^6 Pas for distal flow 1.

In each Hawaiian eruption here considered, the evolution of the flow can be effectively modelled with two viscosities: an initial low viscosity for the first 1/2–1 day and a second higher

viscosity for the rest of the flow. A first implication of this result is that the calculated apparent viscosities are heavily weighted towards the viscosity of the flow front as new lava is continuously erupted at the vent with the same initial low viscosity (with the exception of the Mauna Loa eruption where the crystallinity of the erupted magma increased with time, Lipman and Banks 1987). This is supported by Kilburn and Lopes (1991) who stated that lava flow lengthening depends mainly on the flow front dynamics, and by numerical simulations based on the conditions at the flow front (Wadge et al. 1994).

It is well known that crystallisation increases the viscosity of lava (e.g. Pinkerton and Norton 1995; Costa 2005) and that the degree of undercooling affects the crystallisation rate (e.g. Wadge et al. 1994). We have found that the advance of some lava flows can be modelled with just two lava viscosities, but as magma crystallises its bulk viscosity increases and there will be a continuum of viscosities in a lava flow. To explore how a lava flow might be approximated by two viscosities despite this continuum, we consider the Einstein-Roscoe equation which relates the viscosity of a suspension with the crystal content:

$$\mu = \mu_o \left(1 - \frac{\phi}{\phi_m}\right)^{-2.5} \quad (21)$$

where μ_o is the melt viscosity, Φ is the crystal content and Φ_m is the maximum packing fraction. For instance, if we assume Φ_m=0.66, then for Φ up to 0.3, the viscosity increases less than an order of magnitude and we can approximate the initial advance of the lava with a single viscosity. As crystallisation continues, the viscosity will increase markedly because of the sensitivity of viscosity to quite small changes in crystallinity at relatively high crystal contents. The viscosity could reach a second relatively constant (but higher) viscosity when crystallisation slows down because near-equilibrium conditions are reached.

Cashman et al. (1999) found that the cooling of Hawaiian lava flows is stronger during the first few kilometres. Crisp et al. (1994) noted that the downstream crystallinity increase of the 1984 Mauna Loa lava flow was mainly due to the microlite crystallisation, with crystal growth and nucleation rates being much higher in the first stage of flow due to strong disequilibrium. Cooling in lava-feeding fire fountains and degassing at the vent are likely causes of strong initial disequilibrium (Sparks and Pinkerton 1978). Crisp et al. (1994) determined nucleation and growth rates of 3×10^{-8} to 1×10^{-7} cm s^{-1} and 1×10^{4} to 3×10^{5} cm^{-3} s^{-1}, respectively, noting that these values are higher than previous estimates for other volcanic rocks based on crystal size distributions. Following the approach of Crisp et al. (1994) the microlite content as a function of time is estimated from:

$$\phi_{mic}(t) = \left[1 - \exp\left(-\kappa_v J G^3 t^4\right)\right](1 - \phi_o) \quad (22)$$

where Φ_{mic} is the microlite content as a volume fraction, κ_v is a shape factor, ranging from 0.6 to 6 in the 1984 Mauna Loa crystals, J is the nucleation rate, G is the growth rate, t is time and Φ_o is the volume fraction of microphenocrysts (Kirpatrick 1981 and Cashman 1990). For example, in 12 h (comparable to the typical duration of the first stage in our fitting of flow regimes to eruption data), the microlite content increases to 0.4, using the low-end values of G and J given by Crisp et al. (1994) and an initial microphenocryst content of 0.1. With longer time scales (up to 2 days; the longest duration of stage 1 in our fits) and different G and J values (in the range of estimates of Crisp et al. 1994), the total crystal content could be up to 1 (i.e. holocrystalline), which is clearly too crystalline but supports the idea of a fast increase in viscosity during the initial stages.

The same authors suggest that the inferred lower crystallisation rates in the second stage of the flow could be common in lava flows as a consequence of new near-equilibrium conditions being reached after initial degassing and cooling. In addition, the release of latent heat can reduce the subsequent crystallisation once near equilibrium conditions are reached after the initial burst of microlite formation. Other studies have shown that after a certain distance from the vent, the temperature and crystallinity of the lava flow remain more or less constant because of thermal insulation due to the crust, as in the 1783–1784 Laki eruption (rubbly flow, Guilbaud et al. 2007), or a lava tube (a morphology not analysed in this work) as in the 1859 Mauna Loa eruption (Riker et al. 2009). Initially, the crust is thin enough and it does not affect the dynamics of the flow but if the crust thickens substantially it may control the flow advance as in the YSC regime.

Yield strength magnitudes

The calculated yield strength values are in the order of 10^5–10^6 Pa for all lava flows where yield strength models (YSC or YS) fit better than the Newtonian model. This is similar to the yield strengths estimated for lava domes by others authors using scaling arguments (Blake 1992) or the morphology of the flows, together with analogue experiments (Fink and Griffiths 1998).

To test the importance of the yield strength on the dynamics of lava flows, we compared the mean flow velocity and height from Eq. (6) for Newtonian and Bingham flows with a range of yield strength values, in a similar way to Dragoni et al. (1986). We set β=5°, ρ=2,500 kg/m^3 and μ=10^6 Pa s and used effusion rates from 0.1 to 1,000 m^3/s. Figure 9a and b shows that with increasing effusion rates the velocity and height of the Bingham flow are more similar to the Newtonian case. For yield strengths up to 10^4 Pa, H and u are very close to the Newtonian case (σ_y=0) when the effusion rate is higher than 5 m^3/s.

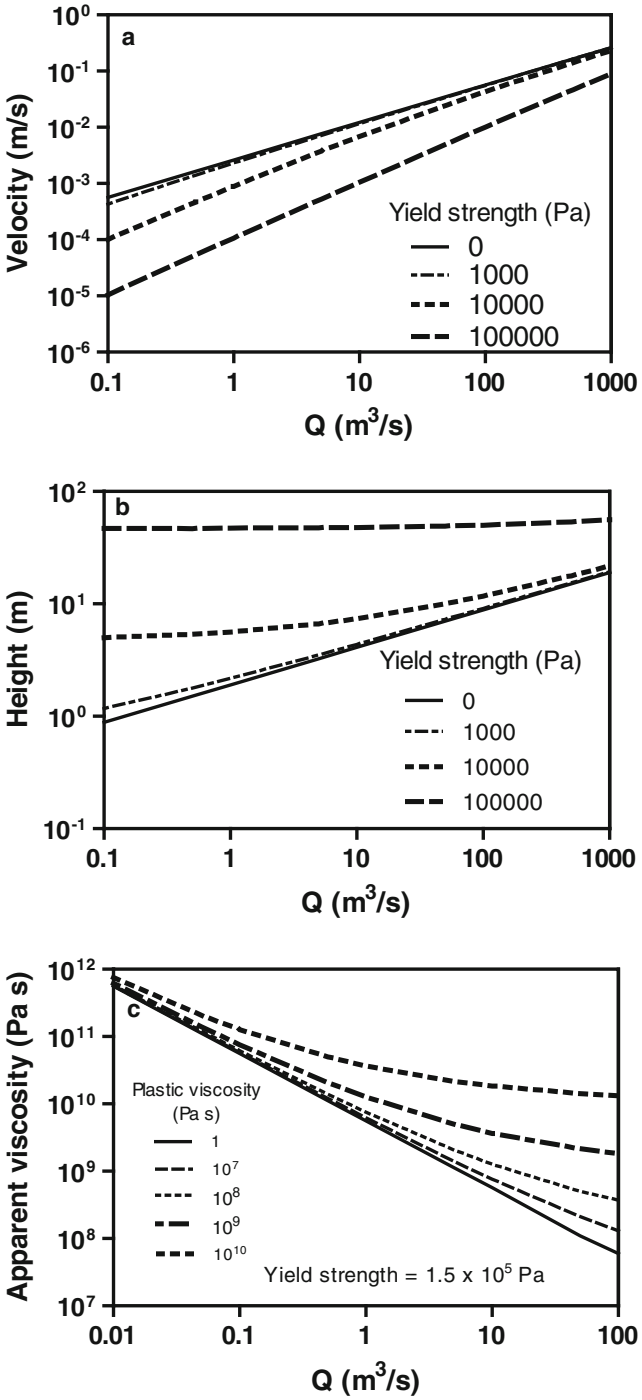

Fig. 9 Velocity (**a**) and flow height (**b**) as a function of effusion rate for a lava flow using a two-dimensional model (Eq. 6) with an internal viscosity of 10^6 Pas, a slope of 5°, and a flow width of 200 m. *Different curves* represent different yield strengths. **c** Calculated apparent viscosities (using Jeffrey's equation) for a lava with a yield strength of 1.5×10^5 Pa, β=15°, ρ=2,500 kg/m^3 and W=200 m. *Different lines* represent different plastic viscosities

Figure 9c shows the calculated apparent viscosity (using H and velocity u with the Jeffrey's equation: $\mu=H^2\rho g\sin\beta/3u$) for a lava with a yield strength of 1.5×10^5 Pa (mean value for the Colima and Santiaguito lava flows) for different plastic viscosities (μ in Eq. 1), using β=15°, ρ=2,500 kg/m^3 and W=200 m. For plastic viscosities up to 10^8 Pas, and effusion rates in the range of 0.5–10 m^3/s (typical of Colima and Santiaguito lava flows), the apparent viscosities are all of order 10^9–10^{10} Pas, in accordance with viscosities estimated by Navarro-Ochoa et al. (2002) and Harris et al. (2004) for these eruptions. This supports our conclusion that the flow front advance rate for these two lava flows was controlled by the yield strength, and that the calculated apparent viscosities reflect the yield strength of the lavas.

If a flow is controlled by the yield strength of a growing crust, the retarding force of the crust should be much bigger than the viscous force of the core:

$$\sigma_c \frac{\delta}{H} >> \mu\dot{\gamma} \tag{23}$$

If we scale $\dot{\gamma}\sim\frac{\overline{u}}{H-\delta}$, the relationship can be written as:

$$\sigma_c >> \mu\frac{\overline{u}}{\delta}\left(\frac{H}{H-\delta}\right) \tag{24}$$

Using Eq. (6), we can evaluate the minimum value of σ_c necessary for it to dominate over the viscous stresses of the core, for a given μ, β, W and effusion rate. For example, using a slope of 5°, a flow width of 200 m, a core viscosity of 10^6 Pa s and a flow rate of 10 m^3/s, the yield strength dominates for $\sigma_c >> 2\times10^4$ Pa after 1 day ($\delta\sim0.3$ m) or $\sigma_c >> 4\times10^3$ Pa after 10 days ($\delta\sim0.9$ m). If we use an effusion rate of 100 m^3/s, the yield strength value required for it to dominate is larger: $\sigma_c >> 1\times10^5$ Pa for 1 day and $\sigma_c >> 5\times10^4$ after 10 days. This analysis shows that short-lived eruptions and high effusion rates favour a viscous control of the flow, as is the case with the Hawaiian eruptions, where an effusion rate higher than 100 m^3/s is typical and the duration of the flows typically is in the range of 1–10 days. Lower effusion rates as in the Etna eruptions or long-lived episodes as in the Lonquimay eruption, favour a crustal control as confirmed by our previous analysis. In addition, higher effusion rates will tend to reduce heat loss per distance flowed (Harris and Rowland 2009), thus preventing the growth of an external crust and, consequently, favouring a viscous control of the flow.

These analyses suggest that yield strengths of about ~10^5 Pa or greater are necessary in the crust or core of the flow in order for yield strength to dominate over the viscosity in resisting the lava flow advance. The tensile strength of solid crystalline rocks is in the order of 10^6 to 10^7 Pa (e.g., Iverson 1992; Rocchi et al. 2004). Crusts undergoing cooling may be even weaker than these values because of internal tensile stresses created by cooling (Dance et al. 2001). Stresses higher than 10^5–10^6 Pa will thus cause the rock to fracture, reducing the effective strength of the lava, and this can explain the consistency of the yield strength values we determined from flow front advance data.

Conclusions

In this study, we investigated the front evolution of simple lava flows on a slope using three rheologically simple models based on scaling arguments. The models were tested with previously published data of front evolution from diverse eruptions and our analysis suggests that for short-lived basaltic eruptions with high effusion rate, the best fit of the data is with the use of two viscosities (Newtonian case). For mafic eruptions with lower effusion rates (Etna eruptions) or long duration andesitic eruptions (Lonquimay eruption, Chile), the flow is controlled by the yield strength of a growing crust. Finally, for very crystalline blocky lavas (Colima, Santiaguito), the flow is controlled by its core yield strength. If our method is used as a predictive tool, the calculated advance rates should be considered as maxima, given that we did not consider down-flow mass loss such as branching, channel overflow or avalanching of blocks from flow fronts.

The viscosities from our analysis are in the same range as previous studies using field measurements on the same lavas. In all cases where the yield strength of the core or a growing crust, rather than a Newtonian viscosity, control the flow front advance rate, the yield strength value is in the order of 10^5 Pa, which is similar to yield strength estimates for lava domes (Blake 1992). We suggest that the consistency of yield strength (~10^5 Pa) is because larger stresses cause fracturing of very crystalline magma, which limits values of yield strength, since a layer of fractured rock clasts has effectively no strength. Furthermore, we used a 2D analysis of a Bingham fluid flow on a slope to conclude that, for lower yield strength values, the flow is controlled mainly by its plastic viscosity and the lava can be effectively modelled as Newtonian.

Our analysis provides a simple tool to evaluate the main controlling forces in the evolution of a lava flow, as well as the magnitude of its rheological properties. The method is effective for eruptions of different compositions and conditions and may be useful to predict the evolution of lava flows if the effusion rate is known.

Acknowledgements AC thanks the financial support given by CONICYT Chile through the Presidente de la Republica scholarship and FONDAP project 15090013. ACR was supported by a Royal Society University Research Fellowship, and RSJS thanks the support of a European Research Council Advanced Grant.

References

Balmforth NJ, Craster RV (2000) Dynamics of cooling domes of viscoplastic fluid. J Fluid Mech 422:225–248

Behncke B, Neri M (2003) The July–August 2001 eruption of Mt. Etna (Sicily). Bull Volcanol 65:461–476

Blake S (1992) Viscoplastic models of lava domes. In: Fink JH (ed) Lava flows and domes: emplacement mechanisms and hazard implications. Springer, Berlin, pp 88–128

Borgia A, Linneman S, Spencer D, Morales LD, Brenes J (1983) Dynamics of lava flow fronts, Arenal volcano, Costa Rica. J Volcanol Geotherm Res 19:303–329

Cashman K (1990) Textural constraints on the kinetics of crystallization of igneous rocks. Rev Mineral Geochem 24:259–314

Cashman C, Thornber C, Kauahikaua J (1999) Cooling and crystallization of lava in open channels, and the transition of Pahoehoe Lava to `A`a. Bull Volcanol 61:306–323

Castruccio A, Rust AC, Sparks RSJ (2010) Rheology and flow of crystal-bearing lavas: insights from analogue gravity currents. Earth Planet Sci Lett 297:471–480

Coltelli M, Proietti C, Branca S, Marsella M, Andronico D, Lodato L (2007) Analysis of the 2001 lava flow eruption of Mt. Etna from three-dimensional mapping. J Geophys Res 112:F02029. doi:10.1029/2006JF000598

Costa A (2005) Viscosity of high crystal content melts: dependence on solid fraction. Geophys Res Lett 32:L22308. doi:10.1029/2005GL024303

Crisp J, Cashman KV, Bonini JA, Hougen SB, Pieri DC (1994) Crystallization history of the 1984 Mauna Loa lava flow. J Geophys Res 99:7177–7198

Dance M, Hancock PL, Sparks RSJ, Wallman A (2001) Fracture and surface crust development in a Holocene lava flow on the island of Tenerife, Canaries. J Struct Geol 23:165–182

Del Negro C, Fortuna L, Herault A, Vicari A (2008) Simulations of the 2004 lava flow at Etna volcano using the magflow cellular automata model. Bull Volcanol 70:805–812

Dragoni M, Tallarico A (1994) The effect of crystallisation on the rheology and dynamics of lava flows. J Volcanol Geotherm Res 59:241–252

Dragoni M, Tallarico A (1996) A model for the opening of ephemeral vents in a stationary lava flow. J Volcanol Geotherm Res 74:39–47

Dragoni M, Bonafede M, Boschi E (1986) Downslope flow models of a Bingham liquid: implications for lava flows. J Volcanol Geotherm Res 30:305–325

Favalli M, Harris AJL, Fornaciai A, Pareschi MT, Mazzarini F (2009) The distal segment of Etna's 2001 basaltic lava flow. Bull Volcanol 72:119–127

Fink JH, Griffiths RW (1998) Morphology, eruption rates and rheology of lava domes: insights from laboratory models. J Geophys Res 103:527–546

Fink JH, Zimbelman JR (1986) Rheology of the 1983 royal gardens basalt flows, Kilauea volcano, Hawaii. Bull Volcanol 48:87–96

Gay EC, Nelson PA, Armstrong WP (1969) Flow properties of suspensions with high solid concentrations. AICHE J 15:815–822

Griffiths RW, Fink JH (1993) Effects of surface cooling on the spreading of lava flows and domes. J Fluid Mech 252:667–702

Guest JE, Kilburn CRJ, Pinkerton H, Duncan AM (1987) The evolution of lava flow-fields: observations of the 1981 and 1983 eruptions of Mount Etna, Sicily. Bull Volcanol 49:527–540

Guilbaud MN, Blake S, Thordarson T, Self S (2007) Role of Syn-eruptive cooling and degassing on textures of lavas from the AD 1783-1784 Laki eruption, South Iceland. J Petrol 48:1265–1294

Harris AJL, Rowland SK (2001) FLOWGO: a kinematic thermo-rheological model for lava flowing in a channel. Bull Volcanol 63:20–44

Harris AJL, Rowland SK (2009) Effusion rate controls on lava flow length and the role of heat loss: a review. In: Thordarson T, Self S, Larsen G, Rowland SK, Hoskuldsson A (eds) Studies in volcanology. The legacy of George walker. Special publications of IAVCEI. Geological Society, London, pp 33–51

Harris AJL, Flynn LP, Matías O, Rose W, Cornejo J (2004) The evolution of an active silicic lava flow field: an ETM + perspective. J Volcanol Geotherm Res 135:147–168

Harris AJL, Dehn J, Calvari S (2007) Lava effusion rate definition and measurement: a review. Bull Volcanol 70:1–22

Hulme G (1974) The interpretation of lava flow morphology. Geophys J R Astron Soc 39:361–383

Huppert HE (1982) The propagation of two-dimensional and axisymmetric viscous gravity currents over a rigid horizontal surface. J Fluid Mech 121:43–58

Huppert HE, Shepherd JB, Sigurdsson H, Sparks RSJ (1982) On lava dome growth, with application to the 1979 lava extrusion of the Soufrière of St. Vincent. J Volcanol Geotherm Res 14:199–222

Ishihara K, Iguchi M, Kamo K (1992) Numerical simulation of lava flows on some volcanoes in Japan. In: Fink JH (ed) Lava flows and domes: emplacement mechanisms and hazard implications. Springer, Berlin, pp 174–207

Iverson RM (1992) Lava domes modelled as brittle shells that enclose pressurized magma, with application to Mount St. Helens. In: Fink JH (ed) Lava flows and domes: emplacement mechanisms and hazard implications. Springer, Berlin, pp 47–69

Kerr RC, Lyman AW (2007) Importance of surface crust strength during the flow of the 1988–1990 andesite lava of Lonquimay Volcano, Chile. J Geophys Res 112:B03209. doi:10.1029/2006JB004522

Kilburn CRJ, Lopes R (1991) General patterns of flow field growth: Aa and blocky lavas. J Geophys Res 96:19721–19732

Kirpatrick R (1981) Kinetics of crystallization of igneous rocks. Rev Mineral Geochem 8:321–398

Lipman PW, Banks NG (1987) Aa flow dynamics, Mauna Loa. In: Decker W, Wright TL, Stauffer PH (eds) Volcanism in Hawaii. US Geol Surv Prof Paper no. 1350, pp 1527–1567

Lister JR (1992) Viscous flows down an inclined plane from point and line sources. J Fluid Mech 242:631–653

Miyamoto H, Sasaki S (1997) Simulating lava flows by an improved cellular automata method. Comput Geosci 23:283–292

Moore HJ (1987) Preliminary estimates of the rheological properties of 1984 Mauna Loa Lava. In: Decker W, Wright TL, Stauffer PH (eds) Volcanism in Hawaii.US Geol Surv Prof Paper no. 1350,pp 1569–1588

Moreno H, Gardeweg M (1989) La erupción reciente en el complejo volcanico Lonquimay (diciembre 1988-), Andes del Sur. Rev Geol Chile 16:93–117

Naranjo JA, Sparks RSJ, Stasiuk MV, Moreno H, Ablay GJ (1992) Morphological, structural and textural variations in the 1988–1990 andesite lava of Lonquimay Volcano. Chile. Geol Mag 129:657–678

Navarro-Ochoa C, Gavilanes-Ruíz JC, Cortés-Cortés A (2002) Movement and emplacement of lava flows at Volcán de Colima, México: November 1998–February 1999. J Volcanol Geotherm Res 117:153–167

Pinkerton H, Norton GE (1995) Rheological properties of basaltic lavas at sub-liquidus temperatures: laboratory and field measurements on lavas from Mount Etna. J Volcanol Geotherm Res 68:307–323

Pinkerton H, Sparks RSJ (1976) The 1975 sub-terminal lavas, Mount Etna: a case history of the formation of a compound lava field. J Volcanol Geotherm Res 1:167–182

Pinkerton H, Wilson L (1994) Factors controlling the lengths of channel-fed lava flows. Bull Volcanol 56:108–120

Riker J, Cashman K, Kauahikaua J, Montierth C (2009) The length of channelized lava flows: insight from the 1859 eruption of Mauna Loa Volcano, Hawai'i. J Volcanol Geotherm Res 183:139–156

Rocchi V, Sammonds PR, Kilburn CRJ (2004) Fracturing of Etnean and Vesuvian rocks at high temperatures and low pressures. J Volcanol Geotherm Res 132:137–157

Ryerson FJ, Weed HC, Piwinskii AJ (1988) Rheology of subliquidus magmas 1. Picritic compositions. J Geophys Res 93:3421–3436

Sparks RSJ, Pinkerton H (1978) Effect of degassing on rheology of basaltic lava. Nature 276:385–386

Takagi D, Huppert HE (2010) Initial advance of long lava flows in open channels. J Volcanol Geotherm Res 195:121–126

Tallarico A, Dragoni M (1999) Viscous Newtonian laminar flow in a rectangular channel: application to Etna lava flows. Bull Volcanol 61:40–47

Vicari A, Ciraudo A, Del Negro C, Herault A, Fortuna L (2009) Lava flow simulations using discharge rates from thermal infrared satellite imagery during the 2006 Etna eruption. Nat Hazard 50:539–550

Wadge G, Young P, McKendrick I (1994) Mapping lava flow hazards using computer simulation. J Geophys Res 99:489–504

Walker GPL (1973) Lengths of lava flows. Phil Trans R Soc London A 274:107–118

Wolfe EW, Neal CA, Banks NG, Duggan TJ (1988) Geologic observations and chronology of eruptive events. In: Wolfe EW (ed) The Puu Oo Eruption of Kilauea Volcano, Hawaii: Episodes 1 through 20, January 3, 1983, through June 8, 1984. US Geol Surv Prof Pap no. 1463, pp 1–97

Zhou JZQ, Fang T, Luo G, Ulherr PHT (1995) Yield stress and maximum packing fraction of concentrated suspensions. Rheol Acta 34:544–561